Open access • Journal Article • DOI:10.1039/C9CE01449G

Halogen bonding (HaB) in E–I···X–M systems: influence of the halogen donor on the HaB nature — Source link

Silvia Dortez, Francisco Fernández-Palacio, Jesús Damián, Carlos Gaiteiro ...+3 more authors

Institutions: University of Alcalá, Spanish National Research Council

Published on: 03 Feb 2020 - CrystEngComm (The Royal Society of Chemistry)

Topics: Halogen bond, Halogen and Covalent bond

ARTICLE

Halogen Bonding (HaB) in E-I ··X-M systems: Influence of the halogen donor in the HaB nature.

Received 00th January 20xx,
Accepted 00th January 20xx

DOI: 10.1039/x0xx00000x

Silvia Dortéz,[a] Francisco Fernández-Palacio,[a] Jesús Damián,[a] Carlos Gaiteiro,[a] Javier Ramos,*[,b] Pilar Gómez-Sal *[,a] and Marta E. G. Mosquera*[,a]

New halogen bonded networks containing the organometallic complexes $[Ru(CN^tBu)_4(X)_2]$ (X = Cl, Br, I) have been prepared. Two different types of halogen donor have been explored, I_2 and IC_6F_4I, to study the influence of the halogen bond donor in the parameters and the nature of the interaction. We have performed a combined experimental and theoretical study. In the results, the species with IC_6F_4I as halogen bond donor show weaker interactions, as evidenced by the geometrical parameters and by the DFT calculations. In fact, it was not possible to isolate the HaB network containing the complex $[Ru(CN^tBu)_4(I)_2]$ and IC_6F_4I. Furthermore, the studies show that the interaction for the iodine has a higher covalent component than for the IC_6F_4I.

Introduction

Halogen bonding (HaB) is an interaction established between the electrophilic side of a covalently bound halogen, considered the halogen donor, and an electron rich atom or molecule that behaves as a Lewis base.[1] This type of interactions is under the umbrella of the so called σ-hole interactions that have also been described for other p-block elements.[2] This highly directional interaction has awakened a particularly high interest. The number of studies on HaB keeps increasing, motivated not only by the intrinsic interest in learning more about how molecular systems are organized, but also, due to its clear influence in many properties and processes.[3] As such, halogen bonding can play a leading role in molecular recognition processes,[4] crystal engineering,[5] as well as in reactivity and even catalisys.[6] Furthermore, its impact in some physicochemical properties[7] and biological systems[8] justifies the high interest awakened by HaB.

Since the beginning of the studies of HaB, the nature of this interaction and the different components that are present in the energy balance has been a topic of great debate.[1,9] Although the electrostatic forces account for the most important part of the interaction, other components such as polarizability, dispersion and exchange forces can affect to an important extent the properties of the HaB in a particular system. Certainly, to have a deeper understanding of the nature of this interaction may lead to a higher level of control when using it to tailor properties and reactivities.[10] In particular, the possibility of controlling the forces present depending on the species that compose the interaction would be very useful. In this respect, many studies have been performed for organic systems, however, metallic species have been significantly less explored.*

In our group we are focused in the study of HaB interactions between halide ligands (M-X, M = transition or main group metal) and suitable HaB donors to generate supramolecular networks.[11,12] We have explored the compounds $[Ru(CNR)_4(X)_2]$, as acceptors and the halogen molecules I_2 and Br_2 as donors.[12,13] These studies have led to the isolation of a whole series of supramolecular networks where $[Ru(CN^tBu)_4(X)_2]$ (X = Cl, Br, I) units and Y_2 (Y = Br, I) molecules are linked by HaB. The analysis of the networks formed allowed us to establish a comparison of the arrangements depending on the HaB acceptor, which was in line with the observations made by others.(Ding et al.) Moreover, in these $[Ru(CNR)_4(X)_2]$ complexes unusual substitution reactions promoted by the presence of the HaB with the X_2 units were observed.[12]

In order to enlarge our knowledge about Ru-halide complexes, in this work we have extended the studies to the iconic halogen donor IC_6F_4I to investigate the different arrangements generated and the nature of the interaction in comparison to when X_2 is the HaB donor. Although other authors have analyzed the nature of the halogen bond as a function of the halide ligands with I_2 as halogen donor,[22] the combined study of the influence of the HaB donor and acceptor has not previously been reported for Ru compounds.

[a] *Departamento de Química Orgánica y Química Inorgánica, Instituto de Investigación en Química "Andrés M. del Río" (IQAR) Universidad de Alcalá, Campus Universitario, 28871-Alcala de Henares, Madrid. Spain. E-mail: martaeg.mosquera@uah.es.*

[b] *BIOPHYM, Department of Macromolecular Physics, Instituto de Estructura de la Materia, IEM-CSIC, C/ Serrano 113 bis, 28006 Madrid, Spain. E-mail: j.ramos@iem.cfmac.csic.es.*

† Footnotes relating to the title and/or authors should appear here.

Electronic Supplementary Information (ESI) available: [details of any supplementary information available should be included here]. See DOI: 10.1039/x0xx00000x

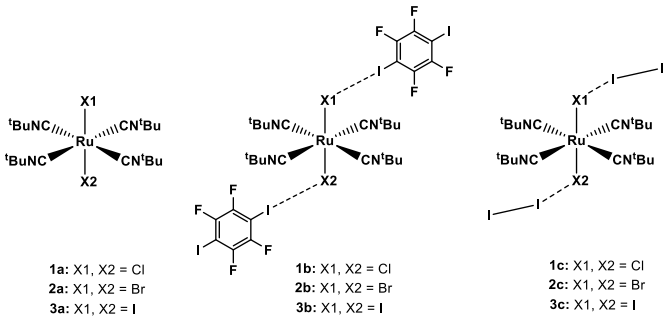

Scheme 1. Structures and acronyms of the studied complexes**.**

These studies have allowed us to isolate the new HaB species **1b** and **2b** (*Scheme 1*). Furthermore, Density Functional Theory (DFT) calculations have been performed to investigate the structural and electronic features of the complexes to gain a better understanding of the HaB nature as a function of the donor and acceptor in **1b**-**3b** and **1c**-**3c**. These detailed theoretical calculations have permitted us to rationalise the observed experimental results and to find significant differences in the nature of the halogen bonding interaction depending on the HaB donor.

Results and discussion

Synthesis and structural characterization

The derivatives $[Ru(CN^tBu)_4(X)_2]$ (X = Cl (**1a**), Br (**2a**)) and $[Ru(CN^tBu)_4(X)_2]\cdot I_2$ (X = Cl (**1c**), Br (**2c**), I (**3c**)) were prepared as described in our previous work.[12,13] Compounds **1c**-**3c**, present HaB interactions between the halogen molecule and the metal complex as depicted in Scheme 1. To synthetized the new species $[Ru(CNR)_4(X)_2]\cdot IC_6F_4I$, we dissolved equimolecular amounts of $[Ru(CNtBu)_4(X)_2]$ (**1a**-**3a**) and IC_6F_4I in CH_2Cl_2. The expected co-crystals were obtained for the compounds $[Ru(CNR)_4(Cl)_2]$ (**1a**) and $[Ru(CNR)_4(Br)_2]$ (**2a**), however for the derivative with the iodide ligand no co-crystal could be isolated. We also studied the competitive behaviour of $[Ru(CN^tBu)_4Cl_2]$ and $[Ru(CN^tBu)_4I_2]$ by adding IC_6F_4I to a mixture containing both. In this case, only the cocrystal $[Ru(CNR)_4Cl_2]\cdot IC_6F_4I$, **1b**, was isolated.

The structures for **1b** and **2b** were confirmed by single crystal X-ray diffraction studies. The crystal structures for $[Ru(CNR)_4(X)_2]\cdot IC_6F_4I$ (X = Cl (**1b**), Br (**2b**)) are isostructural. In the packing, the metal complexes are interacting with the IC_6F_4I generating chains in the shape of ladders. In both cases, there is a significant reduction of the X···I distance in comparison to the sum of the van der Waals radii (table 1),[14] although the reduction is less than the one observed when the HaB is established with I_2 (**1c**: 3.110(2) Å[12] and **2c**: 2.9931(10) Å[13]). These chains are organized in layers via H bonding interactions between two dichloromethane molecules and the halide ligand. The Ru-X distances are similar to the ones in the complexes without the interaction.[11,12] However for the IC_6F_4I fragment, the C-I distances are slightly longer than the free arene, without any interaction, (2.075-2.079 Å).[15] The elongation is more noticeable for the bromide ligand (2.109(12) Å) than the chloride (2.096(4) Å).

Table 1. Experimental bond distances for **1b** and **2b** and its comparison with the van der Waals radii sum

X	X···I d (Å)	X···I-C θ_1 (º)	I···X-Ru θ_2 (º)	Δ (Å)	%
Cl	3.171(7)	175.53(1)	112.16(2)	0.559	15.0%
Br	3.321(2)	172.57(4)	110.20(4)	0.509	13.2%

$R_{Van\ der\ Waals}$: Cl = 1.75 Å; Br = 1.85 Å; I = 1.98 Å; $R_{Van\ der\ Waals}$ Sum: Cl + I = 3.74 Å; Br + I =3,83 Å. Δ and % are defined as the absolute and percentage difference between the observed distance and the sum of VdW radii.

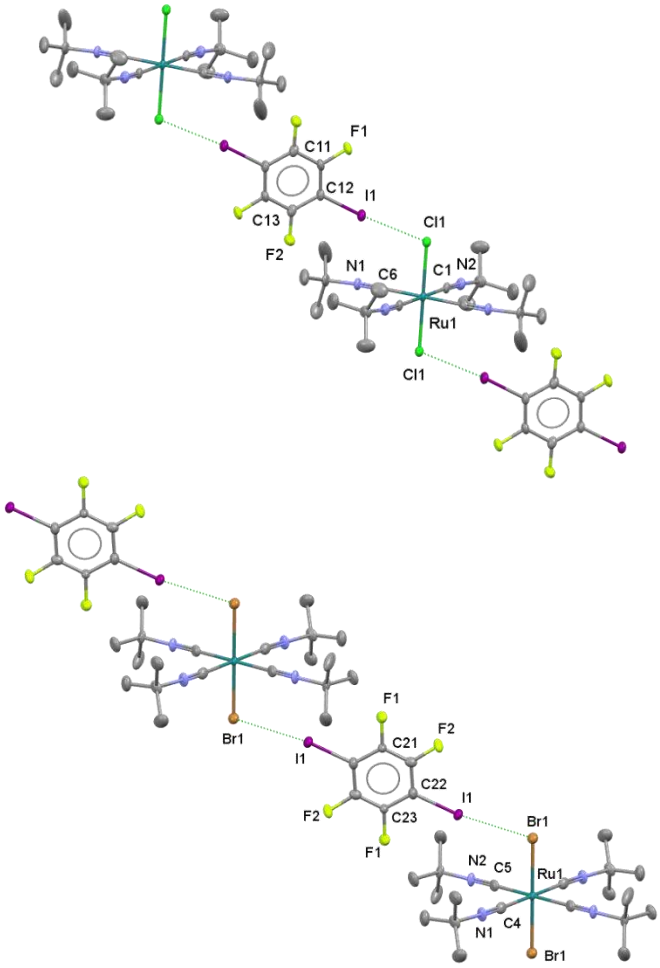

Figure 1. Top: 1D network for **1b**, Ru-Cl 2.4204(11), Cl···I 3.171(7), Cl···I-C 175.53(1). Bottom: 1D network for **2b**, Ru-Br 2.5400(12), Br···I 3.321(2), Br···I-C 172.57(4). Ellipsoids 30% of probability. Bond distances Å; angles (º).

IR spectroscopic studies were performed to analyse the strong stretching band (ν_{st}) for the CN group from the isocyanide ligands as it can give information about the metal electronic

environment. As such, when bonded to a metal electronically poor, isocyanides behave as σ donors and the IR ν_{st}(CN) band shift to higher values. But, when bonded to an electronically richer metal, isocyanides act as π acceptors and the band shifts to lower values due to the increased back-donation from the metal into the π∗ antibonding LUMO orbital. Thus, the analysis of the IR spectra can give a hint of the effect of the formation of the HaB interaction on the metal and a shift to higher values would imply a reduction of electronic density near the metal.[16-18]

For **1a**, the ν_{st}(CN) band shifts from 2131 cm^{-1} to 2143 cm^{-1} in **1b** when the interaction with IC_6F_4I is stablished, and further to 2154 cm^{-1} in the case of **1c** where the HaB with I_2 is present. The same trend is observed for derivatives **2,** with bromide as ligand, for **2a** the band appears at 2132 cm^{-1} which shift to 2139 cm^{-1} for **2b** and to 2161 cm^{-1} in **2c**. These values reflect that the ruthenium is placed in a less electronically rich environment when the HaB is stablished with IC_6F_4I, and this effect is even larger if the I_2 is the halogen donor.

In order to have a further insight on this different behavior depending on the halogen donor, we performed a theoretical study. The initial structures for DFT optimizations of the compounds showed in Scheme 1 were extracted from the crystallographic data.

Geometry optimizations

The optimized geometries for **1a-3a**, **1b-3b** and **1c-3c** are given as PDB files in the supplementary material. The agreement between the optimized and the experimental geometries is quite good (*Figures S.1* to *S.3*). A global comparison is performed by superimposing the structures obtained by X-ray experiments and theoretical calculations (*Fig S.4*), obtaining root mean square deviations values (rmsd) of around 0.70 Å for **1a-3a** and 1.30 Å for **1b-3b** complexes. The larger values for **1b-3b** can be attribute to the largest deviation in the range of 15-18° of the Ru-X-I bend angles. It can be noted that, both Ru-X and X-I distances are, in general, slightly longer that experimental ones. These geometrical differences are attributable to the fact that bond intermolecular interactions and crystal packaging effects are not taken into account in the theoretical calculations. This shows that the theoretical level chosen is suitable for the complexes studied here.

Table 2. Relevant geometrical parameters of the DFT optimized structures in the characterization of halogen bridges. All distances and angles are given in angstroms and degrees, respectively.

Comp	$d_{I\cdots C_6F_4I}$ (Complex)	$d_{I\cdots C_6F_4I}$ (Isolated)	$d_{X\cdots IC_6F_4I}$	X + I $R_{vdWaals}$ Sum	X···I-C_6F_4I angle
1b (X=Cl)	2.084 (2.093)	2.067	3.197 (3.171)	3.730	172.5 (175.6)
2b (X=Br)	2.083 (2.109)	2.067	3.390 (3.321)	3.830	171.6 (172.6)
3b (X=I)	2.083 (n.d)	2.067	3.574 (n.d)	3.960	170.4 (n.d)
	$d_{I\cdots I}$ (Complex)	$d_{I\cdots I}$ (Isolated)	$d_{X\cdots I\text{-}I}$	X + I $R_{vdWaals}$ Sum	X···I-I angle
1c	2.728	2.656	2.880	3.730	178.4
(X=Cl)	(2.733)		(3.057)		(179.5)
2c (X=Br)	2.744 (2.649)	2.656	2.981 (2.993)	3.830	178.5 (178.0)
3c (X=I)	2.782 (2.729)	2.656	3.079 (3.188)	3.960	178.5 (176.3)

Between parentheses the corresponding experimental values. Van der Waals radii are taken from.[14] n.d (not determined)

From a geometrical point of view, there are several parameters which allow to characterize the interaction between donors and acceptors in halogen bonds.[1] Table 2 collects these parameters to compare the halogen interaction in complexes **1b-3b** and **1c-3c**. Distances I···I in the **1c-3c** adducts are longer respect to the isolated I_2 molecule by 0.07, 0.09 and 0.13 Å for X = Cl, Br and I, respectively. The corresponding elongations in the **1b-3b** adducts are clearly shorter (around 0.02 Å) and independent of the X atom. In both, **1b-3b** and **1c-3c**, the distances between X···I are shorter than the sum of van der Waals radii,[14] although in complexes **1c-3c** are appreciably shorter than in **1b-3b**. A largest deviation of 180° for the X···I···I(C) angle is also observed for **1b-3b** adducts, decreasing the directionality of the halogen bond for these complexes. These geometrical differences suggest a strong halogen interaction in the **1c-3c** adducts, that have I_2 as halogen donor.

Table 3. Relative coordination energies of I_2 and IC_6F_4I donors to the **1a**-**3a** acceptors containing two terminal halogen atoms (X). All energies are given in kcal/mol.

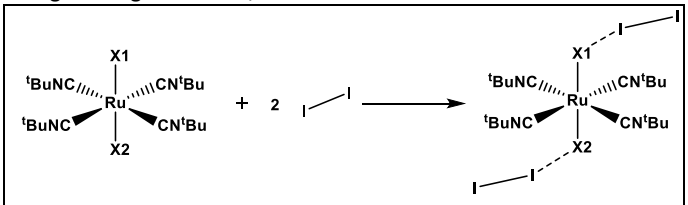

X	ΔE_{elect}[1)]	ΔE_{elect}+ ZPE[2)]	ΔE_{elect}+ ΔH_{corr}[3)]
Cl	-24.2	-23.1	-22.4
Br	-24.3	-23.3	-22.5
I	-25.6	-24.8	-23.8

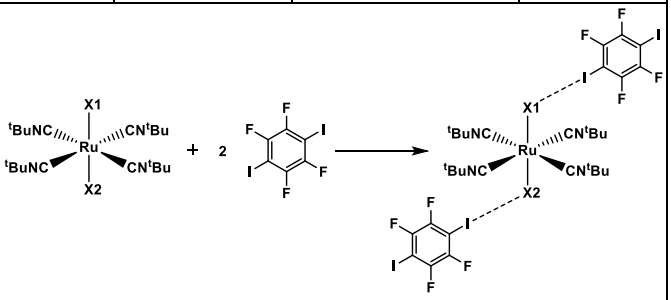

X	ΔE_{elect}[1)]	ΔE_{elect}+ ZPE[2)]	ΔE_{elect}+ ΔH_{corr}[3)]
Cl	-16.7	-15.6	-14.3
Br	-15.4	-14.1	-12.9
I	-15.2	-14.3	-12.8

[1)] ΔE_{elect} is defined as the difference of electronic energies of products and reactants as $\Delta \boldsymbol{E}_{elect} = \boldsymbol{E}_{elect,product} - \sum \boldsymbol{E}_{elect,reactants}$.

[2)] Including zero-point energy (ZPE) and [3)] thermal corrections at 298.15K. All calculations are performed using dichloromethane as implicit solvent (see computational details)

Adduct binding energy

Binding energies for the adducts **1b-3b** and **1c-3c** upon coordination of I-C_6F_4-I and I_2 to the complexes **1a-3a**, respectively, are shown in Table 3. The binding energies of I_2 are greater than those of I-C_6F_4-I donors. The I_2···(I-Ru-I)···I_2 (**3c**) complexes are more stable that its counterparts I_2···(Cl-Ru-Cl)···I_2 (**1c**) by ca. 1.4 kcal/mol. This is in close agreement with the experimental observation that the HaB strength decreases in the order I>Br>Cl according to a decreasing in the polarizability of the halogens.[19] On the contrary, the reverse order is observed for the ligand I-C_6F_4-I, where I-C_6F_4-I···(Cl-Ru-Cl)···I-C_6F_4-I (**1b**) is more stable that **3b** I-C_6F_4-I···(I-Ru-I)···I-C_6F_4-I by *ca*. 1.5 kcal/mol. These differences along with the analysis of geometrical parameters above discussed could indicate a different nature of the bonds between the halogen bond acceptor and donors. Thus, in the following discussion, the bond nature is further analyzed by using molecular electrostatic potential surfaces (MEPs) and quantum theory of atoms-in-molecules (QTAIM).

Molecular electrostatic potential surface (MEPs) and quantum theory of atoms-in-molecules (QTAIM) analysis.

The molecular electrostatic surface potential (MEPs) was calculated to examine the behavior of several inter-atomic regions as proposed by Bader et *al.*.[20] Figure 2 depicts the MEPs on the surface of the molecule ($V_s(r)$) for both I_2 and I-C_6F_4-I halogen bond-donors. It is evident the presence of a positive region (blue color) in the outermost part of the electrostatic surface along the axis of the I-I and I-C bond, respectively, surrounded by a belt of negative electrostatic potential (yellow color). The maximum positive value ($V_{s,\,max}$) of the electrostatic potential is faced to the iodine atoms and correspond to the so-called σ-hole. The I_2 and IC_6F_4I halogen bond-donors present similar spatial range and magnitude ($V_{s,\,max}$ values) suggesting a similar halogen bond donor ability from an electrostatic point of view. The MEP surfaces for the **1a-3a** halogen bond-acceptors are also shown in the Figure 2 The most negative regions of the MEPs are situated along the Ru-X bond (X= Cl, Br and I). In this case, the $V_{s,\,min}$ values are located in the surrounding of the halogen atom bonded to the metal and its value increases following the order Cl < Br < I (red points in Figure 2), whereas the most positive of the MEPs are situated in the equatorial plane of the complex (blue points in Figure 2). From an electrostatic point of view, the most positive electrostatic regions in both halogen bond-donors (I_2 and I-C_6F_4-I) could interact with the most negative regions in the halogen bond-acceptor, following the same order of interaction **1a** > **2a** > **3a** irrespective of the halogen bond-donor. This clearly does not agree with the geometrical parameters and adduct binding energies for the **1b-3b** and **1c-3c** complexes, above discussed.

To gain more detailed information about the differences between the halogen bond-donors for a given acceptor, QTAIM analysis of the complexes **1b-3b** and **1c-3c** were also performed. The QTAIM analysis exposes bond critical points (BCP, critical points of type (3, -1)) between the halogen linked to the Ru and the iodine atom in halogen bond-donors, as shown in Figure . Certain properties of the charge density at these BCPs have been proposed to study the nature of the non-covalent interactions (see Table 4). [21,22]

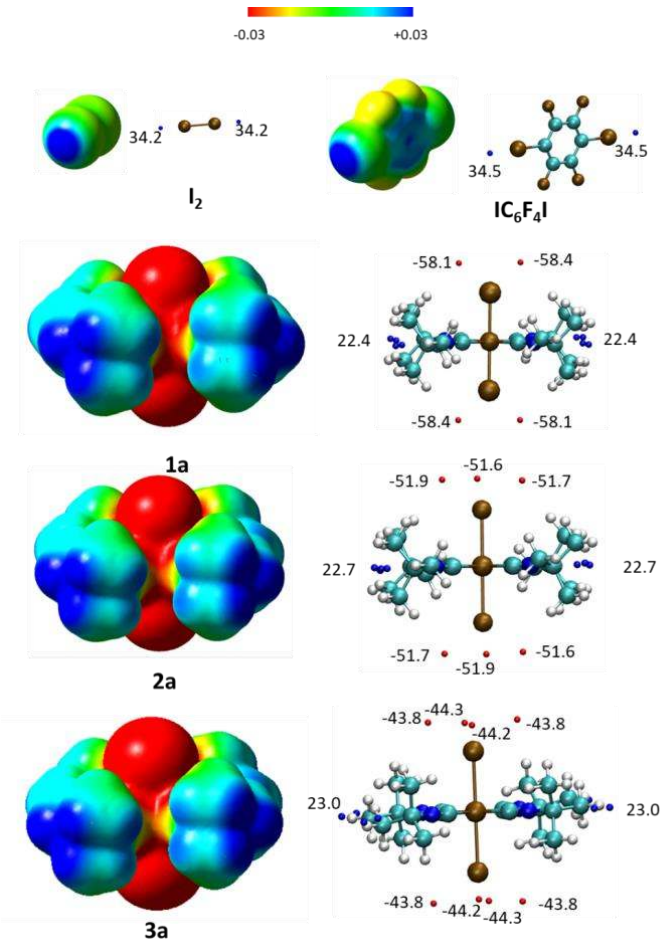

Figure 2: Computed electrostatic potentials ($V_s(r)$) mapped on the 0.001 electron/bohr^3 electron density of the donors (**1a-3a**) and acceptors (I_2 and IC_6F_4I). The value of 0.001 electron/bohr^3 was proposed by Bader as it encompasses approx. 97% of the molecule's electronic charge [8]. Negative and positive $\mathbf{V_s(r)}$ values are red and blue, respectively. The location of the most positive ($V_{s,\,max}$) and most negative ($V_{s,\,min}$) electrostatic potentials are shown as red and blue points, respectively, along with their values in kcal/mol at the right of the figure.

Firstly, electron density at the critical points in I_2 complexes (**1c-3c**) are larger than those found in IC_6F_4I ones (**1b-3b**). This can be interpreted as stronger halogen bonds for **1c-3c**. Furthermore, the order for electron density at the BCP in I_2 complexes is I>Br>Cl, in concordance with the adduct binding energy (Table 3). The reverse order is observed in the IC_6F_4I complexes **1b-3b**. The values for $\rho(r_c)$ in systems forming weak H bonds can be used as reference, being in the range of 0.024-0.036 $Å^{-3}$.[23] Thus, the halogen bonds here studied seems to be one order of magnitude larger for **1c-3c** complexes (0.229-0.249 $Å^{-3}$). The ratio between the potential and the kinetic energy densities ($|V(rc)|/G(rc)$) can be used to characterize the nature of the interactions, thus values less than 1.0 are typical of electrostatic interaction and values larger than 2.0 are interpreted as covalent interactions.[21] Similarly, negatives $H(r_c)$ values are indicative of covalent interactions. Clearly, BCPs in **1b-3b** compounds have an electrostatic character. In contrast, **1c-3c** complexes are characterized by negative values of $H(r_c)$ and ($|V(r_c)|/G(r_c)$) values between 1.0 and 2.0, showing a more covalent character. In addition, the character covalent follows the order **3c>2c>1c**, in agreement with the adduct binding energies.

Table 4. Properties of the electron density from QTAIM analysis of the two halogen bond critical points found in complexes **1b**-**3b** and **1c**-**3c**. The properties are the electron density ($\rho(r_c)$, in $Å^{-3}$), the Laplacian of the electron density ($\nabla\rho(r_c)$, in $Å^{-5}$) the kinetic energy density ($G(r_c)$, in kj/mol), the potential energy density ($V(r_c)$, in kj/mol) and total energy density ($V(r_c)$, in kj/mol).

Com	CPs	$\rho(r_c)$	$\nabla\rho(r_c)$	$G(r_c)$	$V(r_c)$	$H(r_c)$	$\lvert V\rvert/G$
1b	X1-I1	0.120	1.280	32.0	-29.2	2.8	0.912
(X=Cl)	X2-I2	0.116	1.248	30.9	-28.0	2.9	0.906
2b	X1-I1	0.102	0.973	24.6	-22.7	1.9	0.923
(X=Br)	X2-I2	0.102	0.972	24.6	-22.7	1.9	0.923
3b	X1-I1	0.094	0.802	20.4	-18.9	1.5	0.926
(X=I)	X2-I2	0.094	0.798	20.3	-18.8	1.5	0.926
1c	X1-I1	0.229	1.703	53.5	-60.6	-7.1	1.133
(X=Cl)	X2-I2	0.229	1.703	53.5	-60.6	-7.1	1.133
2c	X1-I1	0.233	1.380	46.9	-56.2	-9.3	1.198
(X=Br)	X2-I2	0.233	1.380	46.9	-56.2	-9.3	1.198
3c	X1-I1	0.249	1.100	42.5	-55.0	-12.5	1.295
(X=I)	X2-I2	0.249	1.100	42.5	-55.0	-12.5	1.295

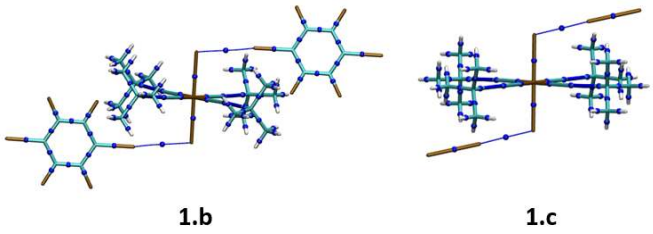

Figure 3. The molecular graph of $[Ru(CN^tBu)_4(Cl_2)]\bullet(2\ IC_6F_4I)$ (**1.b**) and $[Ru(CN^tBu)_4(Cl_2)]\bullet(2I_2)$ (**1.c**) and bond critical points as blue points. The bond paths lines for the Cl···I halogen bond is also shown as blue lines. The 2.b, 3.b, 2.c and 3.c critical points are similar and they are not shown.

Experimental

General Considerations. All manipulations were conducted using Schlenk techniques and at room temperature unless otherwise is stated. All solvents were dried prior to use. NMR spectra were recorded at 400.13 (^{1}H), and 100.62 (^{13}C) MHz on a Bruker AV400. Chemical shifts (δ) are given in ppm using $CDCl_3$ as solvent. ^{1}H and ^{13}C resonances were measured relative to solvent peaks considering TMS δ = 0 ppm. Elemental analyses were obtained on a Perkin-Elmer Series II 2400 CHNS/O analyser. All reagents were commercially obtained and used without further purification. Compounds **1a** and **3a-3c** were prepared as previously reported.[12, 13]

Synthesis of $[Ru(CN^tBu)_4(I)_2]$ (1c). To a solution of $[Ru(CN^tBu)_4(Cl)_2]$ (0.1 g, 0.2 mmol) in 20 mL of MeOH and excess of of NaI were added 0.60 g (4.00 mmol). The solution was stirred overnight. Then the solvent was removed under vacuum and compound **1c** was extracted from the solid residue by adding 20 ml of CH_2Cl_2. The solution was filtered, one third of the solvent removed under vacuum and the solution was stored in the fridge. After one week yellow crystals of **1c** were isolated form the solution. Yield: 78 %, 0.11 g. Elemental analysis $RuC_{20}H_{36}N_4I_2$: cacld (%)*:* C = 34.95; H = 5.28; N = 8.15. Found (%)*:* C = 34.86; H = 5.24; N = 8.33. IR (cm^{-1}, KBr): ν_{st} (CN) 2130 (f).

General procedure for the reaction of $[Ru(CNR)_4(X)_2]$ (1a-3a) and IC_6F_4I. All the reactions were performed by adding the appropriate amount of IC_6F_4I dissolved in 10 mL of CH_2Cl_2 to a solution of compounds **1a-3a** in 10 mL of CH_2Cl_2. After the addition the solution was stirred for 3 hours. The volume of the reaction mixture was reduced to 10 ml under vacuum. The crystalline compounds were isolated from the reaction mixture after a slow evaporation process.

Synthesis of 1b: 0.05 g (0.1 mmol) of **1a**, $[Ru(Cl)_2(CNtBu)_4]$, and IC_6F_4I (0.1 mmol) dissolved in 10 mL of CH_2Cl_2 were added. Yield: 82 %, 0.07 g. Elemental analysis $RuC_{20}H_{36}N_4Cl_2 \cdot IC_6F_4I \cdot CH_2Cl_2$: cacld (%)*:* C = 32.71; H = 3.86; N = 5.65. Found (%)*:* C = 32.55; H = 3.93; N = 5.97. IR (**1b**) (cm^{-1}, KBr): ν_{st} (CN) 2143 (f).

Synthesis of 2b: 0.06 g (0.1 mmol) of **2a**, $[Ru(Br)_2(CNtBu)_4]$, and IC_6F_4I (0.04 gr, 0.1 mmol). Yield: 86 %, 0.08 g. Elemental analysis $RuC_{20}H_{36}N_4Br_2 \cdot IC_6F_4I$: cacld (%)*:* C = 31.38; H = 3.65; N = 5.63. Found (%)*:* C = 31.05; H = 3.83; N = 5.87. IR (**1b**) (cm^{-1}, KBr): ν_{st} (CN) 2139 (f).

Single-Crystal X-ray Structure Determinations of 3a, 1b and 2b. Details of the X-ray experiment, data reduction, and final structure refinement calculations are summarized in Table 3. Single crystals suitable for X-ray diffraction studies were selected for Data collection. The crystals were stuck to a glass fiber using an inert perfluorinated ether oil and mounted in a low temperature N_2 stream 200(2) K, in a Bruker-Nonius Kappa CCD single crystal diffractometer equipped with a graphite-monochromated Mo-Kα radiation (λ = 0.71073 Å), and an Oxford Cryostream 700 unit. The structures were solved by

direct methods (SHELXS-97), using the WINGX package,[24] and completed by subsequent difference Fourier techniques and refined by using full-matrix least-squares against F^2 (SHELXL-97).[25] All non-hydrogen atoms were anisotropically refined. The hydrogen atoms were geometrically placed and left riding on their parent atoms. Absorption corrections were performed with the programs SORTAV (semi-empirical from equivalent).[26] The crystals of **2b·** were not of optimal quality.

Crystallographic data (excluding structure factors) for the structures reported in this paper have been deposited with the Cambridge Crystallographic Data Centre as supplementary publication no. CCDC-1944150 (**3a**) 1944151 (**1b**) CCDC-1944154 (**2b**)]. Copies of the data can be obtained free of charge on application to CCDC, 12 Union Road, Cambridge CB2 1EZ, UK (e-mail: deposit@ccdc.cam.ac.uk).

Table 6. **Crystallographic Data for 3a, 1b and 2b**,

Compound	3a	1b	2b
Formula	$C_{20}H_{36}I_2N_4Ru$	$C_{28}H_{40}Cl_6F_4I_2N_4Ru$	$C_{28}H_{40}Br_2Cl_4F_4I_2N_4Ru$
FW	687.40	1076.21	1165.13
Cryst syst	Monoclinic	Triclinic	Triclinic
Space group	C 2/c	P -1	P-1
a (Å)	17.0495(10)	9.1900(5)	9.3125(4)
b (Å)	9.9661(8)	9.434(2)	9.3992(4)
c (Å)	18.6572(17)	13.143(3)	12.7543(5)
α(°)		88.54(2)	71.7590(10)
β (°)	115.397(6)	69.663(12)	81.883(2)
γ(°)		86.654(16)	80.600(2)
V (Å^3)	2863.8(4)	1066.6(3)	1041.20(8)
F(000)	1336	524	560
μ/mm^{-1}	2.714	2.231	4.076
Z, ρ_c (g.cm^{-3})	4, 1.594	1, 1.675	1, 1.858
2Θ range (°)	3.00-27.52	3.12-27.5	1.69-25.75
Cryst size (mm^3)	0.20 0.32 0.35	0.39 0.30 0.24	0.25 0.1 0.1
Reflns. collected	10233	9023	8243
Ind. Reflns./Rint	3269/0.0505	4846/ 0.0295	3500/0.0445
Data/rest/param	3269/0/124	4846/0/205	3500/0/206
R_1/wR_2 (I>2σ(I))[a]	0.0398/0.0884	0.036/0.0779	0.068/0.2074
R_1/wR_2(all data)[a]	0.0755/0.1056	0.0737/0.0914	0.0817/0.263
$\Delta\rho_{max}/\Delta\rho_{min}$ (eÅ^{-3})	0.845/-1.020	1.257/-1.298	2.205/-2.315
GOF (on F^2)[a]	0.874	0.916	1.138

[a] $R_1 = \Sigma(||F_o| - |F_c||)/\Sigma|F_o|$; $wR_2 = \{\Sigma[w(F_o^2 - F_c^2)^2]/\Sigma[w(F_o^2)^2]\}^{1/2}$; GOF = $\{\Sigma[w(F_o^2 - F_c^2)^2]/(n - p)\}^{1/2}$

Computational details. All the calculations were performed using the M06-2X meta-GGA exchange-correlation functional [27] as implemented within the Gaussian 16 package [28]. This functional has been assessed to reproduce non-covalent interactions,[27] which are important in the complexes shown in *Scheme 1*. Solvation effects were taken into account within the Polarizable Continuum Model (PCM) using the integral equation formalism variant (IEFPCM)[29] for dichloromethane solvent (ε = 8.93). All other parameters for PCM method were kept in their default values in Gaussian16. The improved triple-ζ valence with polarization def2-TZVP basis set was adopted for all atoms. This basis set has proved to give results not too far from the DFT basis set limit at a rather reasonable computational cost.[30] The ultrafine option in Gaussian16 was used for numerical integrations. The structure is converged if the maximum force and maximum displacement are smaller than $4.5x10^{-4}$ a.u and $1.8x10^{-3}$ a.u, respectively. Additionally, the root-mean-square (RMS) force and displacement must be smaller than $3.0x10^{-4}$ a.u and $1.82x10^{-3}$ a.u, respectively. Frequency calculations at 298.15K have been performed both to confirm the absence of imaginary frequencies which indicates that the structure is a local minimum and to calculate zero-point energy (ZPE) and thermal corrections. All inputs and outputs are available upon request to the authors.

Both molecular electrostatic potential surface (MEPs) and quantum theory of atoms-in-molecules (QTAIM) analysis were carried out using MultiWfn code (version 3.4.1).[31] The wave function was obtained from the optimized geometries and then supplied to MultiWfn program. Structural figures were rendered using VMD 1.9.4 visualization package.[32]

Conclusions

New organometallic networks generated by halogen bonding interactions have been prepared using the metal complexes $[Ru(CN^tBu)_4(X)_2]$ (X = Cl, Br, I) as halogen acceptors. The species isolated with IC_6F_4I as halogen bond donor show weaker interactions than when I_2 is the halogen donor, as evidenced by the geometrical parameters and by calculations. The geometric structures were calculated by DFT and are very close to the experimental ones for all studied structures. Some slightly differences are observed in **1b-3b** and **1c-3c** complexes attributed to packing effects in the crystallographic structures, which are not considered in the calculations.

The binding energies of I_2 to **1a-3a** complexes are greater than those of IC_6F_4I donors. The resulting order for I_2 agrees with the observation that the HaB strength decreases from iodide to chloride, I>Br>Cl, in agreement to a decreasing in the polarizability of the halogens. However, the reverse order is obtained for the IC_6F_4I donor, and in fact, it was not possible to isolate experimentally the HaB network containing the complex $[Ru(CN^tBu)_4(I)_2]$ and IC_6F_4I (**3b**).

The analysis of the wave function, using MEPs and QTAIM methods, to investigate the nature of the complexes $[Ru(CNR)_4(X)_2]\cdot IC_6F_4I$ and $[Ru(CNR)_4(X)_2]\cdot I_2$, shown that the nature of the X···I interactions in $[Ru(CNR)_4(X)_2]\cdot I_2$ complexes have a higher degree of covalency than for $[Ru(CNR)_4X_2]\cdot IC_6F_4I$, where the nature of bond seems to be purely electrostatic. The most negative ($V_{s,\ min}$) values, which can be used to characterize the strength of an electrostatic bond between acceptor and donor, indicate the same order than those found for the binding energy in $[Ru(CNR)_4X_2]\cdot IC_6F_4I$ complexes.

Hence the nature of the energy balance involved in the interaction can be tuned by the rational choice of the halogen bond donor. Although the covalent component is much smaller than the electrostatic one, it seems to have an effect in the reactivity of the species formed and for derivatives **1c-3c** an evolution in solution is observed that leads to a halide ligand substitution process,[11,12] while species **1b-2b** are stable in solution.

Conflicts of interest

There are no conflicts to declare.

Acknowledgements

Financial support from Spanish Government (MINECO CTQ2014-58270-R and Factoría de Cristalización-Consolider–Ingenio (CSD2006-00015)), and the Alcalá University, Spain (CCG2018/EXP-038) is gratefully acknowledged. J.R acknowledges financial support through the CSIC (Spain) - Project PIE201860E136.

Notes and references

1 G. Cavallo, P. Metrangolo, R. Milani, T. Pilati, A. Priimagi, G. Resnati, G. Terraneo, *Chem. Rev*., 2016, **116**, 2478; P. Metrangolo, H. Neukirch, T. Pilati and G. Resnati, *Acc. Chem. Res*. 2005, **38**, 386;

2 M. H. Kolaŕ and P. Hobza *Chem. Rev.* 2016, **116**, 5155; P. Politzer, J. S. Murray and T. Clark, *Phys.Chem.Chem.Phys*., 2013, **15**, 11178; L. Brammer, *Faraday Discuss.*, 2017, **203**, 485-507

3 L. C. Gilday, S. W. Robinson, T. A. Barendt, M. J. Lang, B. R. Mullaney and P. D. Beer, *Chem Rev.* 2015, **115**, 7118; M. Tuikka, P. Hirva, K. Rissanen, J. Korppi-Tommolab and M. Haukka, *Chem. Commun.* 2011, **47**, 4499–4501; A. Priimagi, G. Cavallo, P. Metrangolo, G. Resnati, G. *Acc. Chem. Res.* 2013, **46**, 2686; M. Fourmigue, *Struct Bond*, 2008, **126**, 181-207. . N. Ramasubbu, R. Parthasarathy and P. Murray-Rust, *J. Am. Chem. Soc.,* 1986, **108**, 4308; L. Brammer, E. A. Bruton and P. Sherwood, *Cryst. Growth Des.*, 2001, **1**, 277; P. Batail and M. Fourmigue, *Chem. Rev*., 2004, **104**, 537; P. Metrangolo, G. Resnati, T. Pilati and S. Biella, *Halogen Bonding in Crystal Engineering, Springer Berlin/Heidelberg*, 2008, pp. 105-136; P. Metrangolo and G. Resnati, *Science*, 2008, **321**, 918; M. Tuikka, P. Hirva, K. Rissanen, J. Korppi-Tommola and M. Haukka, *Chem Commun*, 2011, **47**, 4499; G. R. Desiraju, P. Shing Ho, L. Kloo, A. C. Legon, R. Marquardt, P. Metrangolo, P. Politzer, G. Resnati and K. Rissanen, *Pure Appl. Chem*., 2013, **85**, 1711–1713; T. Clark, M. Hennemann, J. S. Murray and P. Politzer, *J. Mol. Model.* 2007, **13**, 291-298; V. R. Hathwar, R. G. Gonnade, P. Munshi, M. M. Bhadbhade and T. N. Guru Row, *Cryst. Growth Des*. 2011, **11**, 1855-1862.

4 F. Zapata, A. Caballero, N. G. White, T. D. W. Claridge, P. J. Costa, V. Félix and P. D. Beer, *J. Am. Chem. Soc*., 2012, **134**, 11533; N. L. Kilah, M. D. Wise, C. J. Serpell, A. L. Thompson, N. G. White, K. E. Christensen and P. D. Beer, *J. Am. Chem. Soc*., 2010, **132**, 11893; T. M Beale, M. G. Chudzinski, M. G. Sarwar, M. S. Taylor, *Chem. Soc. Rev.*, 2013, **42**, 1667; M. G. Sarwar, B. Dragisic, S. Sagoo and M. S. Taylor, *Angew. Chem. Int. Ed*., 2010, **49**, 1674; M S. Taylor, *Top Curr. Chem*. 2015, **359**, 27-48; L. González, F. Zapata, A. Caballero, P. Molina, C. Ramírez de Arellano, I. Alkorta and J. Elgero, *Chem. Eur. J.*, 2016, **22**, 1; S. Ruiz-Botella, P. Vidossich, G. Ujaque, E. Peris and P. D. Beer, *RSC Adv.*, 2017, **7**, 11253.

5 C. B. Aakeroy, P. D. Chopade and J. Desper, *Cryst. Growth Des*, 2011, **11**, 5333; C. B. Aakeroy, P. D. Chopade, C. Ganser and J. Desper, *Chem. Commun*., 2011, **47**, 4688; P.Metrangolo, F. Meyer, T. Pilati, G. Resnati and G. Terraneo, *Angew. Chem., Int. Ed.* 2008, **47**, 6114; S. Derossi, L. Brammer, C. A. Hunter and M. D. Ward, *Inorg. Chem*. 2009, **48**, 1666; L. Rajput, G Mukherjee and K. Biradha, *Cryst. Growth Des*. 2012, **12**, 5773; F. Zordan, L. Brammer and P. Sherwood, *J. Am. Chem. Soc* 2005, **127**, 5979 5989; L. Brammer, E. A. Bruton and P. Sherwood, *Cryst. Growth Des.*, 2001, **1**, 277; S. Saha, G. R. Desiraju, *J. Am. Chem. Soc*, 2017, **139**, 1975 ; V. Thangavadivale, P. M. Aguiar, N. A. Jasim, S. J. Pike, D. A. Smith, A. C. Whitwood, L. Brammer and R. N. Perutz, *Chem. Sci*., 2018, **9**, 3767; K. E. Riley and K.-An Tran, *Faraday Discuss*., 2017, **203**, 47-60.

6 F. Kniep, S. H. Jungbauer, Q. Zhang, S. M. Walter, S. Schindler, I. Schnapperelle, E. Herdtweck and S. M. Huber, *Angew. Chem. Int. Ed*., 2013, **52**, 7028; O. Coulembier, F. Meyer and P. Dubois, *Polym. Chem*, 2010, **1**, 434; H. Nakatsuji, Y. Sawamura, A. Sakakura and K. Ishihara, *Angew. Chem. Int. Ed*., 2014, **53**, 1; Y. Wang, J. Wang, G-X Li, G. He and G. Chen, *Org. Lett.*, 2017, **19**, 1442; J-P, Gliese, S. H. Jungbauer and S. M. Huber, *Chem Commun*, 2017, **53**, 12052. D. P. De Sousa, C. Wegeberg, M. S. Vad, S. Morup, C. Frandsen, W. A. Donald and C. J. McKenzie, *Chem. Eur. J.*, 2016, **22**, 3810; T. A. Hamlin, I. Fernandez, and F. M. Bickelhaupt, *Angew. Chem. Int. Ed*. 2019, **58**, 8922; L. Carreras, J. Benet-Buchholz, A. Franconetti, A. Frontera, P. W. N. M. van Leeuwen and A. Vidal-Ferran, *Chem. Commun*., 2019, **55**, 2380; F. Meyer and P. Dubois, *CrystEngComm*, 2013, **15**, 3058; J. Bamberger F. Ostler and O. García-Mancheño; *ChemCatChem*, 2019, 10.1002/cctc.201901215

7 J. Vapaavuori, I. T. S. Heikkinen, V. Dichiarante, G. Resnati, P. Metrangolo, R. G. Sabat, C. G.; Bazuin, A. Priimagi and C. Pellerin, *Macromolecules,* 2015, **48**, 7535; W. Zhu, R. Zheng, Y. Zhen, Z. Yu, H. Dong, H. Fu, Q. Shi, and W. Hu, *J. Am. Chem. Soc*, 2015, **137**, 11038; D. Cinčić, T. Friščić and W. Jones, *Chem. Eur. J.*, 2008. **14**, 747.

8 Z. Xu, Z. Liu, T. Chen, T. T. Chen, Z. Wang, G. Tian, J. Shi, X. Wang, Y. Lu, X. Yan, G. Wang, H. Jiang, K. Chen, S. Wang, Y. Xu, J. Shen and W. J. Zhu, *Med. Chem.* 2011, **54**, 5607; D. A Kraut, M. J. Churchill, P. E. Dawson and D. Herschlag, *ACS Chemical Biology*, 2009, **4**, 269; D. Manna and G. Mugesh, *Cryst. Growth Des*., 2011, **11**, 2279; D. Manna and G. Mugesh *J. Am. Chem. Soc.*, 2012, **134**, 4269; A. R, Voth, F. A. Hays and P. S. Ho, *Proc. Natl. Acad. Sci. USA* 2007, **104**, 6188; T. Wang, P. Yin, Y. Yang, W. Yin, S. Zhang, M. Yang, Y. Qin, Y. Ma, Z. Lei, and He. Ma, *ACS Sustainable Chem Eng*., 2019, **7**, 6295.

9 C. Wang, D. Danovich, Y. Mo and S. Shaik, *J. Chem. Theory Comput*, 2014, **10**, 3726; T. T. T. Bui, S. Dahaoui, C. Lecomte, G. R. Desiraju and E. Espinosa, *Angew. Chem. Int. Ed.* 2009, **48**, 3838; J. Thirman, E. Engelage, S. M. Huber and M. Head-Gordon, *Phys. Chem. Chem. Phys*., 2018, **20**, 905; S. V. Rosokha and A. Traversa, *Phys. Chem. Chem. Phys*., 2015, **17**, 4989.

10 C. B. Aakeroy, T. K. Wijethunga, J. Desper and M. Dakovic, *Cryst. Growth Des*, 2016, **16**, 2662; L. Koskinen, S. Jaaskelainen, P. Hirva and M. Haukka, *Cryst. Growth Des*, 2015, **15**, 1160; W. Borley, B. Watson, Y. P. Nizhnik, M. Zeller, and S. V. Rosokha, J. *Phys. Chem. A* , 2019, **123**, 7113. *cita c)O.Dumele, D. Wu, N. Trapp, N. Goroff, F. Diederich, Org. Lett. 2014, 16,4722–4725. a) D. L. Widner,Q.R.Knauf, M. T. Merucc ´i, T. R. Fritz, J. S. Sauer, E. D. Speetzen, E. Bosch, N. P. Bowling, J. Org. Chem. 2014, 79,6269–6278. C.Cavallotti, P. Metrangolo,F.Meyer, F. Recupero, G. Resnati, J. Phys. Chem. A 2008, 112,9911–9918 Chemsitry :10.1002/chem.201900924

11 F. Vidal, M. A. Dávila, A. San Torcuato, P. Gómez-Sal and M. E. G. Mosquera, *Dalton Trans.*, 2013, **42**, 7074.

12 M. E. G. Mosquera, P. Gómez-Sal, I. Viñas, L. M. Aguirre, C. Mealli and G. Manca, *Inorg Chem*, 2016, **55,** 283.

13 M. E. G. Mosquera, I. Egido, C. Hortelano, M. López-López and P. Gómez-Sal, *Faraday Discussions* 2017, **203,** 257.

14 M. Mantina, A.C. Chamberlin, R. Valero, C.J. Cramer, D.G. Truhlar, *J. Phys. Chem. A*, 2009, **113** 5806.

15 S. Y. Oh, C. W. Nickels, F. Garcia, W. Jones and T. Friscic, *CrystEngComm*, 2012, **14**, 6110.

16 L. B. Kool, M. D. Rausch, M. Herberhold, H. G. Alta, U. Thewalt and B. Honold, *Organometallics*, 1986, **5**, 2465.

17 J. Ruiz, M. E. G. Mosquera, G. García, E. Patrón, V. Riera, S. García-Granda, and F. Van der Maelen, *Angew. Chem. Int. Ed.*, 2003, **42**, 4767-4771.
18 E. J. M de Boer and J. H. Teuben, *J. Organomet. Chem.*, 1979, *166*, 193.
19 P. Politzer, P. Lane, M.C. Concha, Y. Ma, J.S. Murray, *Journal of Molecular Modeling*, 2007, **13**, 305-311.
20 R.F.W. Bader, M.T. Carroll, J.R. Cheeseman, C. Chang, J. *Am. Chem Soc.,* 1987, **109**, 7968-7979.
21 E. Espinosa, I. Alkorta, J. Elguero, E. Molins, *J. Chem. Phys.* , 2002, **117**, 5529–5542.
22 X. Ding, M.J. Tuikka, P. Hirva, V.Y. Kukushkin, A.S. Novikov and M. Haukka, *CrystEngComm*, 2016, **18**, 1987.
23 A. Forni, S. Pieraccini, D. Franchini, M. Sironi, *J. Phys. Chem. A*, 2016, **120**, 9071.
24 L. J. Farrugia, *J. Appl. Crystallogr.*, 1999, ***32***, 837-838.
25 G. M. Sheldrick, *Acta Cryst.*, 2008, **A64**, 112-122.
26 R. H. Blessing, *Acta Cryst Section A: Foundations of Crystallography***,** 1995, **51**, 33-38.
27 Y. Zhao and D.G. Truhlar*, Theoretical Chemistry Accounts*, 2008, **120,** 215-241.
28 M.J. Frisch, G.W. Trucks, H.B. Schlegel, G.E. Scuseria, M.A. Robb, J.R. Cheeseman, G. Scalmani, V. Barone, G.A. Petersson, H. Nakatsuji, X. Li, M. Caricato, A.V. Marenich, J. Bloino, B.G. Janesko, R. Gomperts, B. Mennucci, H.P. Hratchian, J.V. Ortiz, A.F. Izmaylov, J.L. Sonnenberg, Williams, F. Ding, F. Lipparini, F. Egidi, J. Goings, B. Peng, A. Petrone, T. Henderson, D. Ranasinghe, V.G. Zakrzewski, J. Gao, N. Rega, G. Zheng, W. Liang, M. Hada, M. Ehara, K. Toyota, R. Fukuda, J. Hasegawa, M. Ishida, T. Nakajima, Y. Honda, O. Kitao, H. Nakai, T. Vreven, K. Throssell, J.A. Montgomery Jr., J.E. Peralta, F. Ogliaro, M.J. Bearpark, J.J. Heyd, E.N. Brothers, K.N. Kudin, V.N. Staroverov, T.A. Keith, R. Kobayashi, J. Normand, K. Raghavachari, A.P. Rendell, J.C. Burant, S.S. Iyengar, J. Tomasi, M. Cossi, J.M. Millam, M. Klene, C. Adamo, R. Cammi, J.W. Ochterski, R.L. Martin, K. Morokuma, O. Farkas, J.B. Foresman, D.J. Fox, *Gaussian 16* Rev. B.01, in, Wallingford, CT, 2016.
29 J. Tomasi, B. Mennucci and R. Cammi, *Chem. Rev*, 2005, **105**, 2999-3094.
30 F. Weigend, *Phys.Chem.Chem.Phys*, 2006, **8**, 1057-1065.
31 T. Lu and F. Chen, *J. Comp. Chem*. , 2012, **33**, 580-592
32 W. Humphrey, A. Dalke and K. Schulten, *J. Molec. Graphics*, 1996, **14**, 33-38.

